crystals

MDPI

Article

Expired Glucosamine Drugs as Green Corrosion Inhibitors for Carbon Steel in H_2SO_4 Solution and Synergistic Effect of Glucosamine Molecules with Iodide Ions: Combined Experimental and Theoretical Investigations

Lijuan Feng *, Shanshan Zhang, Yan Zhou, Rongkai Pan, Hongchen Du, Fangfang Liu and Yongqi Yang

Shandong Engineering Research Center of Green and High-value Marine Fine Chemical, Weifang University of Science and Technology, Weifang 262700, China
* Correspondence: ljfeng@alum.imr.ac.cn; Tel.: +86-0536-5107638

Abstract: Glucosamine is a natural drug widely used for treating osteoarthritis and is usually left until it expires, which will cause a waste of resources if treated as garbage. However, its molecule contains many heteroatoms, entitling it to be a potential corrosion inhibitor. In this investigation, the corrosion inhibition activities of two types of expired glucosamine drugs (glucosamine hydrochloride and glucosamine sulfate) on carbon steel were estimated by electrochemical methods in the acidic solution. The results demonstrated that the glucosamine drugs were mixed-type corrosion inhibitors. Glucosamine hydrochloride could inhibit the carbon steel corrosion more significantly than that of sulfuric style at the same glucosamine content, suggesting a possible synergistic effect of glucosamine molecules with halide ions. Then, the co-adsorption behaviors of glucosamine sulfate with iodide ions were studied by experimental research, as well as theoretical investigations. The results indicated that the inhibition effect could be significantly enhanced when the glucosamine drug was utilized in combination with iodide ions. The electronic structures played a critical role in the synergistic inhibition of glucosamine drugs and iodide ions. Neutral molecules could interact with the metallic surface vertically through the amino and carbonyl groups, while protonated molecules were able to adsorb on it in parallel with the help of multiple functional groups. Since glucosamine molecules would be protonated and positively charged in the acidic solution, they were difficult to adsorb on the solid surface with metallic cations. When the iodide ions were presented, they preferentially adsorbed on the carbon steel surface and induced it to be negatively charged. Therefore, protonated glucosamine molecules could adsorb on the metallic surface using iodide ions as a bridge and form a protective film to mitigate the carbon steel corrosion.

Keywords: expired drug; glucosamine; carbon steel; green corrosion inhibitor; acidic solution

Citation: Feng, L.; Zhang, S.; Zhou, Y.; Pan, R.; Du, H.; Liu, F.; Yang, Y. Expired Glucosamine Drugs as Green Corrosion Inhibitors for Carbon Steel in H_2SO_4 Solution and Synergistic Effect of Glucosamine Molecules with Iodide Ions: Combined Experimental and Theoretical Investigations. *Crystals* **2023**, *13*, 205. https://doi.org/10.3390/cryst13020205

Academic Editor: Helmut Cölfen

Received: 3 January 2023
Revised: 19 January 2023
Accepted: 19 January 2023
Published: 23 January 2023

1. Introduction

Glucosamine, a kind of natural hexosamine sugar found in the human body, is a non-toxic green compound which can stimulate chondrocytes to produce proteoglycan and improve their recovery ability [1,2]. However, the human body's capability to synthesize glucosamine decreases with aging, which results in many health problems, such as bone and joint inflammation. Thus, two main types of salts viz glucosamine sulfate $[(C_6H_{13}NO_5)_2{\cdot}H_2SO_4]$ and glucosamine hydrochloride ($C_6H_{13}NO_5{\cdot}HCl$) are widely used for the therapy of osteoarthritic patients. In addition, they are also added in health care products by food enterprises as a nutrient for strengthening muscles and bones [3,4]. Therefore, many families have numerous reservations, and lots were left expired. If these expired drugs are treated as garbage, it will not only cause a waste of resources, but also have some unpredictable ecological impacts. Therefore, it is necessary to find new solutions to recycle these expired medicines.

Corrosion inhibitors are a category of agents that can significantly mitigate metal corrosion in a small amount and are widely applied in the petroleum industry, chemical industry, and other fields [5]. The molecule of a corrosion inhibitor usually deserves multi-ring structures, unsaturated bonds, or atoms with large electronegativity, which enables it to interact with the metal via these functional groups or heteroatoms to form a protective film on the metallic surface and suppress its corrosion [5–8]. Nowadays, numerous corrosion inhibitors have been developed, but lots of them are forbidden due to their detrimental effects on the environment. It has been a trend to design and use green, environmental-friendly agents [9,10]. Among them, pharmaceutical products undergo a variety of biological experiments and safety tests, which have been considered as a major branch of green corrosion inhibitors [6,11]. Amino acids, vitamins, and quinolones have all been reported to be able to inhibit metal corrosion [6,12]. Glucosamine molecule contains many atoms with lone pair electrons, entitling it a potential corrosion inhibitor [13]. However, there is still no report on its application in metal protection against corrosion.

Meanwhile, it should be noted that these pharmaceutical agents are not designed to be corrosion inhibitors and the corrosion protection effect on metals may not be ideal. Thus, other compounds often need to be utilized together to enhance their corrosion inhibition effect. Previous investigations have implied that the corrosion inhibition properties of organic compounds are greatly improved by the addition of appropriate halide ions and their synergy increases following the sequence of $Cl^- < Br^- < I^-$ [14,15].

Therefore, corrosion inhibition activities of two expired glucosamine drugs, namely, glucosamine sulfate (GS) and glucosamine hydrochloride (GH), were investigated by potentiodynamic polarization (PDP) and the electrochemical impedance spectrum (EIS) in the acid medium. Iodide ions were added to enhance the inhibition effect. Then, the synergistic mechanism between the glucosamine sulfate and iodide ions was analyzed based on theoretical investigations. This study aims to evaluate the anti-corrosion behaviors of expired glucosamine drugs and to find a strategy to strengthen the corrosion inhibition effect; furthermore, to provide an experimental and theoretical reference for designing new expired pharmaceutical corrosion inhibitors.

2. Materials and Methods

2.1. Materials Preparation

The two types of glucosamine drugs were both expired for more than 1 year. They packed well before the experiments. Glucosamine hydrochloride medicine was produced by Jiangsu Zhengda Qingjiang Pharmaceutical Co., Ltd. Each tablet weighted 0.950 g and contained 3.48 mmol glucosamine. Glucosamine sulfate was purchased from Yongxin Pharmaceutical Industry Co., Ltd. Each tablet weighted 0.415 g and contained 1.09 mmol glucosamine. Since both drugs were slow-release products, after obtaining the appropriate amount of agent by the weight method, they were dissolved in the corrosive medium for 24 h before each experiment to ensure their stable content in the solution.

The corrosive medium used in the study was 0.5 mol L^{-1} H_2SO_4 solution, prepared with 98 wt% sulfuric acid, as well as bi-distilled water.

The electrode (10 mm × 10 mm × 5 mm) utilized in the electrochemical experiment was processed from R235 carbon steel supplied by Yangzhou Xiangwei Machinery Co., Ltd. (Yangzhou, China). Its composition was obtained by the spark discharge atomic emission spectrometric method in the light of the standard GB/T 4336-2016 and was listed in Table 1. The electrode was welded with copper wire at one end and sealed with epoxy resin, where only an exposed surface (1 cm^2) was left for testing. Before each experiment, it was ground to 1000 # step-by-step with abrasive paper, cleaned, and dried with cold air.

Table 1. Composition of the carbon steel electrode.

Content	C	Mn	P	S	Si	Fe
Amount (wt%)	0.16	0.45	0.04	0.05	0.03	Balance

2.2. Electrochemical Measurements

The electrochemical analysis was conducted on the working station (CORRTES, CS310) using the traditional three-electrode system, where a carbon rod served as the auxiliary electrode and a saturated calomel electrode for reference. An open circuit potential (OCP) measurement was carried out for 1 h before each test to make sure the stable corrosion state of the electrode sample. The potentiodynamic scanning was performed from −0.25 V to +0.25 V concerning OCP at a speed of 1 mV s^{-1}. The EIS data were obtained from 100,000 Hz to 0.01 Hz at OCP. The signal used was an alternating current and the perturbation amplitude was set to be 10 mV. The experiments were all conducted at room temperature.

2.3. Computational Details

Gaussian 09 package was employed for the quantum chemical calculations. Geometry optimizations were conducted under the hybrid density functional theory (DFT) framework based on the Lee-Yang-Parr (B3LYP) exchange-correlation functional theory, using the 6-31G(d,p) basis set. During the optimization process, the COSMO model was utilized to introduce the effect of the solvent (water). The Forcite module in the Materials Studio 2019 software (Community) was applied for molecular dynamics simulations. The simulation model consisted of a metal surface, a layer of corrosion inhibitor solution, and a vacuum with a thickness of 30 Å. The metal surface was Fe(110), which contained five layers of iron atoms. It has been proved that the metal suffers from hydrogen evolution corrosion in an acidic solution and is prone to form cations, which causes the solid surface to be positively charged and easy to attract anions [16–18]. Thus, in the model, to study the synergistic effect of glucosamine and iodide ions, 3 I^- was firstly added to the Fe(110) surface. In total, 222 water molecules, 1 glucosamine molecule, 4 H^+, and 2 SO_4^{2-} were used to simulate 0.5 mol L^{-1} H_2SO_4 solution with corrosion inhibitor, where appropriate counterions (H^+, K^+) were added or removed to maintain the charge balance of the simulation system. Since the glucosamine molecule had combined with 1 H^+ after it was protonated, the number of free H^+ was reduced to 3. The molecular interaction was described by COMPASS and was conducted using the NVT ensemble at 298 K with Nosé-Hoover thermostat to control the temperature. The time step was 1 fs, and each system ran for 1000 ps to reach the equilibrium state.

3. Results and Discussion

3.1. Corrosion Inhibition Activities of Expired Glucosamine Drugs on Carbon Steel

3.1.1. PDP

Figure 1 depicted the PDP curves of carbon steel electrodes in the H_2SO_4 solution with different concentrations of expired GS or GH. Since there are 2 glucosamine units in a GS molecule but only 1 in the GH, the molar amount of the GS added was half of the GH to ensure equal glucosamine content. Compared with the blank system (0.5 mol L^{-1} H_2SO_4 solution without corrosion inhibitors, hereinafter same), the cathodic curves shifted towards low current density after adding the expired drugs, indicating that the addition of glucosamine led to a reduction in the electrode corrosion rate [19]. In order to determine the corrosion inhibition influence of glucosamine drugs more clearly, the corrosion potential (E_{corr}), the corrosion current density (i_{corr}), the anodic Tafel slope (β_a), and the cathodic Tafel slope (β_c) could be obtained by fitting the PDP data via the Tafel extrapolation method [20]. The corrosion inhibition efficiency *IE* was calculated according to the formula below [20,21]:

$$IE\ (\%) = [(i^0_{corr} - i_{corr})/i^0_{corr}] \times 100\% \quad (1)$$

where i^0_{corr} and i_{corr} were the corrosion current densities for the uninhibited and inhibited electrodes, respectively. The fitting results were listed in Table 2.

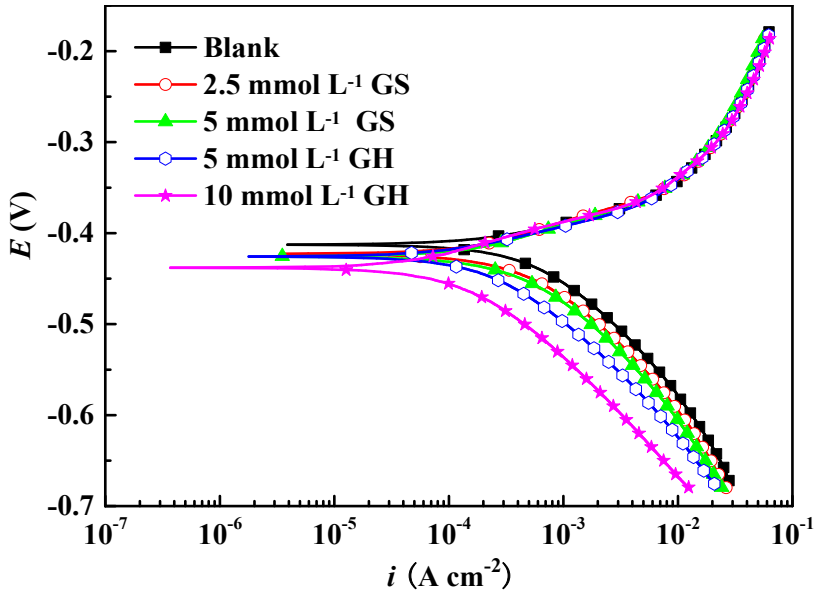

Figure 1. PDP curves of the electrodes in 0.5 mol L^{-1} H_2SO_4 solution without and with various amounts of glucosamine salts.

Table 2. Tafel fitting results of the electrodes in 0.5 mol $L^{-1}H_2SO_4$ solution without and with various amounts of glucosamine salts.

Inhibitor	β_a (mV dec^{-1})	$-\beta_c$ (mV dec^{-1})	i_{corr} (mA cm^{-2})	E_{corr} (mV)	*IE* (%)
Blank	76	121	0.667	−413	/
2.5 mmol L^{-1} GS	74	120	0.427	−423	36.0
5 mmol L^{-1} GS	75	122	0.370	−426	44.5
5 mmol L^{-1} GH	74	122	0.298	−426	55.3
10 mmol L^{-1} GH	72	119	0.119	−438	82.2

According to Figure 1 and Table 2, the i_{corr} decreased with the increasing glucosamine addition, implying that the inhibitor molecules adsorbed on the metallic surface were increased and the corrosion protective effect of the drug became stronger [22]. Furthermore, it can be noted that the *IE* of GS was much lower than that of GH at the same glucosamine content, which might be ascribed to the synergistic inhibition of glucosamine drugs and halide ions. Although E_{corr} got more negative, it is visible that there were hardly any variations in β_a or β_c. Thereby, the glucosamine drugs were mixed-type corrosion inhibitors and their inhibition activities were induced by a coverage effect rather than cathodic electrochemical inhibition [18,22].

3.1.2. EIS

Figure 2 showed the EIS of carbon steel electrodes in the solution with different concentrations of expired GS or GH. Based on the Bode plots (Figure 2b), there was only one time constant for the EIS of the electrode in the corrosive medium, either with or without corrosion inhibitors. Thus, only one irregular capacitive semicircle appeared in the Nyquist moiety (Figure 2a); yet a small inductive arc was visible in the low-frequency part. The capacitive arc corresponded to the electrochemical corrosion process of the electrode, whereas the radius of the capacitive arc indicated its corrosion properties. The larger the radius was, the more difficult the electrochemical corrosion occurred. The inductive arc was induced by the continuous desorption of corrosion products and/or inhibitors from the electrode surface [7,23]. Therefore, the EIS data could be fitted with the equivalent electrical circuit (EEC) in Figure 3 and the fitting results were collected in Table 3. R_s stood

for the solution resistance, R_{ct} the charge transfer resistance, C the capacitance of the electric double layer, R_L the inductive resistance, and L the inductance. Due to the continuous generation of corrosion products, the electrode surface was rough, and the capacitive arc did not fit well with the theoretical model; thus, CPE was employed to replace the capacitive element C. Its value was assessed by the following equations [24,25]:

$$Z_{CPE} = Y^{-1}(2\pi j f_{max})^{-n} \quad (2)$$

$$C = Y(2\pi f_{max})^{n-1} \quad (3)$$

where f_{max} denoted the frequency with the largest value of the impedance imaginary part.

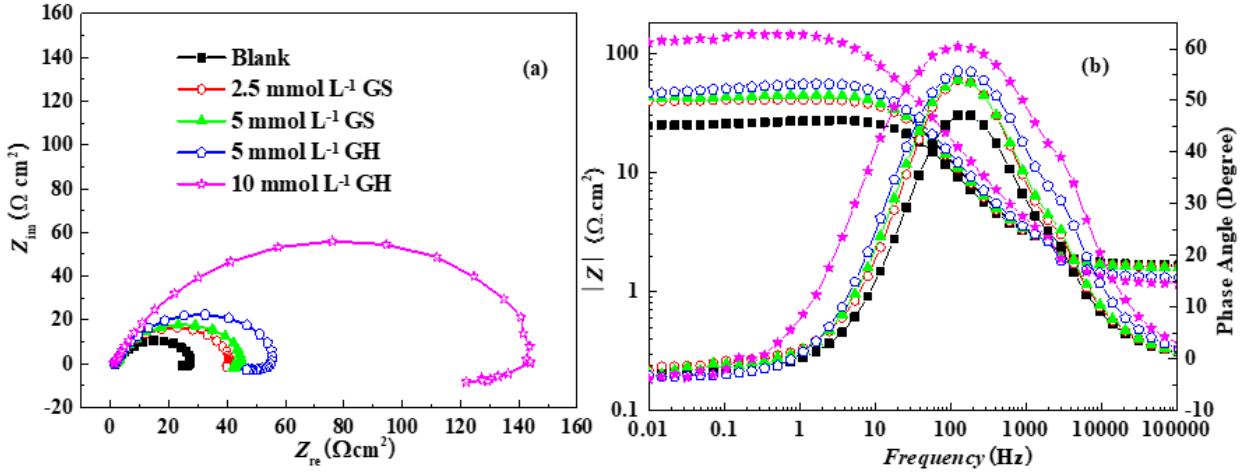

Figure 2. EIS of the electrodes in 0.5 mol L^{-1} H_2SO_4 solution without and with various amounts of glucosamine salts: (**a**) Nyquist diagram; (**b**) Bode plots.

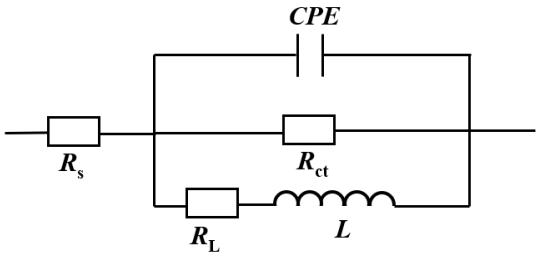

Figure 3. EEC to fit the EIS data for the electrodes in 0.5 mol L^{-1} H_2SO_4 solution without and with various amounts of glucosamine salts.

Table 3. EIS fitting results for the electrodes in 0.5 mol L^{-1} H_2SO_4 solution without and with various amounts of glucosamine salts.

Inhibitor	R_s(Ω cm^2)	$CPE-Y$ (μ Ω^{-1} cm^{-2} S^n)	$CPE-n$	R_{ct} (Ω cm^2)	R_L (Ω cm^2)	L (H cm^2)
Blank	1.67	643	0.76	30.5	121	7.68
2.5 mmol L^{-1} GS	1.64	535	0.77	45.1	142	10.1
5 mmol L^{-1} GS	1.61	482	0.78	51.7	186	11.9
5 mmol L^{-1} GH	1.31	415	0.78	60.5	233	75.5
10 mmol L^{-1} GH	1.14	352	0.77	167.8	699	128

In view of Figure 2 and Table 3, after the addition of the expired glucosamine drug (either GS or GH), the impedance modulus and R_{ct} of the electrode increased relative to the blank system, while $CPE-Y$ representing the capacitive properties decreased. Furthermore,

such a trend got more obvious as the drug amount increased. These results suggested that the amount of glucosamine molecules adsorbed on the electrode surface increased with their increasing concentration; thus, the double layer got thicker, and the carbon steel corrosion was suppressed. It is noteworthy that R_s decreased in the presence of glucosamine drugs, which was due to the fact that GS and/or GH were dissociated to certain ions (such as H^+, SO^{4-}, Cl^-), reducing the dielectric constant of the solution [25,26]. Meanwhile, the protonation of glucosamine molecules in the acidic solution also led to the decline of the solution resistance [27]. Consistent with the PDP results, the impedance modulus and R_{ct} of the carbon steel sample were much larger in the solution with GH than that in the corrosive medium with GS of the same amount by glucosamine, which once again demonstrated that the glucosamine drug might have a synergistic adsorption effect with halide ions. Therefore, it was necessary to study the co-adsorption behaviors of the glucosamine molecules and halide ions.

3.2. Synergistic Corrosion Inhibition Effect of GS with KI

3.2.1. PDP

Previous investigations have confirmed that organic corrosion inhibitors often have synergistic adsorption with halide ions, and this effect is the most significant in iodide ions [14,15]. In order to determine the synergism of glucosamine molecules with halide ions and to further promote the application of expired glucosamine drugs as corrosion inhibitors, various concentrations of iodide ions were employed in the corrosive media and the co-adsorption of iodide ions with 2.5 mmol L^{-1} GS was studied. The results indicated that 2.5 mmol L^{-1} GS had the best protective performance on the carbon steel sample at the iodide ion concentration of 0.75 mmol L^{-1}. Above this value, the corrosion efficiency would decrease (Figure S1). For the purpose of clearly demonstrating the combined corrosion inhibition behaviors of glucosamine and iodide ions, the PDP curves of carbon steel electrodes in the acidic solution with various corrosion inhibitor formulations were illustrated in Figure 4. The fitting results were collected in Table 4.

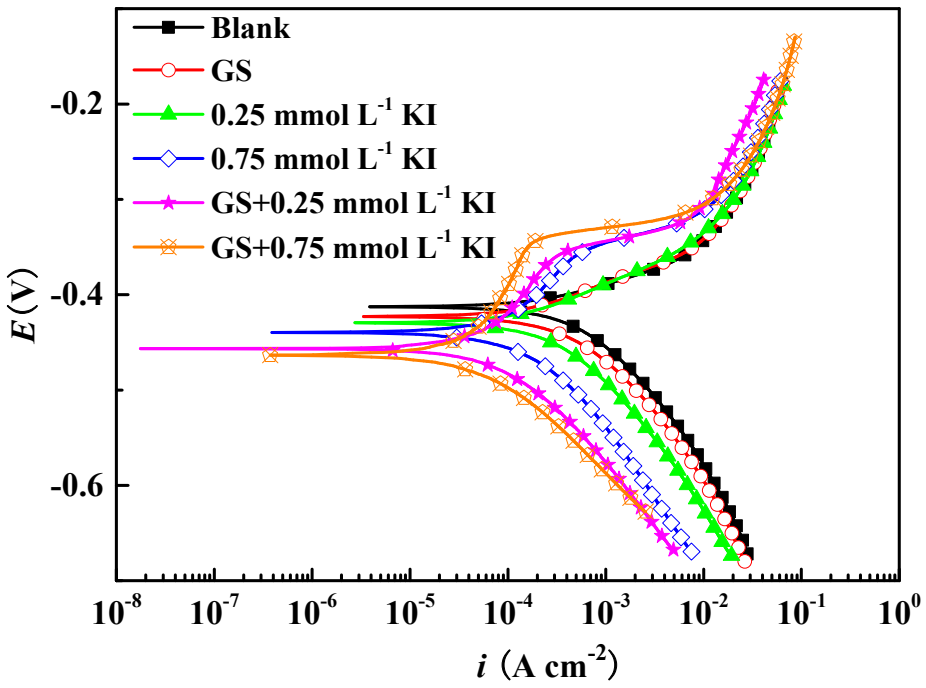

Figure 4. PDP curves of the electrodes in 0.5 mol L^{-1} H_2SO_4 solution without and with different corrosion inhibitor formulations.

Table 4. Tafel fitting results of the electrodes in 0.5 mol L^{-1} H_2SO_4 solution without and with different corrosion inhibitor formulations.

Inhibitor Formulation	β_a (mV dec^{-1})	$-\beta_c$ (mV dec^{-1})	i_{corr} (mA cm^{-2})	E_{corr} (mV)	*IE* (%)	*S*
Blank	76	121	0.667	−413	/	/
GS	74	120	0.427	−423	36.0	/
0.25 mmol L^{-1} KI	78	119	0.304	−429	54.4	/
0.75 mmol L^{-1} KI	90	118	0.109	−439	83.7	/
GS + 0.25 mmol L^{-1} KI	154	118	0.081	−457	87.8	1.24
GS + 0.75 mmol L^{-1} KI	257	119	0.059	−464	91.2	1.02

It is evident that the addition of KI or GS caused the cathodic curve to move towards the low current density; as a result, the corrosion electrochemical reaction rate of the electrode was reduced [28]. The alteration of the anodic curve was very small when GS or 0.25 mmol L^{-1} KI was added alone. However, such a situation was changed when the concentration of KI was increased to 0.75 mmol L^{-1} or KI was applied in combination with GS. Not only did the whole polarization curves shift to the direction of the lower current density, but also the shape of the anodic branches was transformed. The anodic polarization curve presented three different regions: at the potential slightly exceeding OCP, the current density increased slowly; then a potential plateau appeared; finally, above about −0.3 V, it returned to the polarization behavior similar to the sample in the blank system. This phenomenon was closely related to the variation of the electrode surface state. In the acidic solution, the metal corrosion occurred and a large number of positively charged metallic cations were enriched on the solid surface. Thereby, protonated glucosamine molecules could adsorb on the metallic surface, but very difficult [16–18]. In contrast, iodide ions were easy to adsorb on the solid surface through coulombic action because of their opposite charge with the metallic cations. The adsorption of iodide ions led to the reduction in the carbon steel corrosion, but the effect was very limited if its amount was not large enough. Thus, it could hardly change the corrosion behavior of the metal and the shape of the polarization curve was not altered. However, the covered sites by iodide ions increased with the increasing KI addition, and their corrosion inhibition activities to the carbon steel got more significant. In the presence of GS, an obvious co-adsorption emerged. The interaction of glucosamine molecules with the solid surface was strongly enhanced with iodide ions as the mediator, which could form an anti-corrosion layer and effectively inhibit the metal corrosion. When the amount of the iodide ions was increased to about 0.75 mmol L^{-1}, their co-adsorption achieved the best with the highest *IE* of 91.2%. The synergism of corrosion inhibitors and halide ions could be measured by the synergistic coefficient S_I, which was calculated by the following formula [29–31], as showed in Table 4:

$$S_I = (1 - I_{1+2})/(1 - I'_{1+2}) \quad (4)$$

where $I_{1+2} = (I_1 + I_2) - I_1 I_2$. I_1, I_2 and I'_{1+2} were the corrosion inhibition efficiencies of the halide ions and organic corrosion inhibitors, and in the presence of halide ions and organic corrosion inhibitors, respectively. $S_I > 1$ suggests a synergistic corrosion inhibition effect between organic compounds and halide ions; meanwhile, $S_I < 1$ indicates an antagonism between the two species [14,32]. From Table 4, S_I of 2.5 mmol L^{-1} GS and 0.25 mmol L^{-1} KI was 1.24, indicating significant synergism between them. S_I of 2.5 mmol L^{-1} GS and 0.75 mmol L^{-1} KI was 1.02, which might be attributed to their co-adsorption being close to the maximum at this concentration, and there was a certain deviation in the calculation of the synergistic coefficient.

3.2.2. EIS

Figure 5 exhibited the EIS of carbon steel electrodes in the acidic solution without and with different corrosion inhibitor formulations. It can be observed that the EIS behavior

of the electrode in the system with 0.25 mmol L^{-1} KI was similar to that in the blank solution, either with GS or without. There was a suppressed capacitive arc in the Nyquist diagram (Figure 5a) with a small inductance in its low-frequency region. Yet, the inductive arc got much weaker. This might be attributed to the fact that iodide ions and ferrous cations deserved opposite charges, which retarded the dissociation of metal ions from the solid surface. Moreover, the addition of corrosion inhibitor formulations induced the high phase region of Bode plots (Figure 5b) wider, indicating that the charge transfer got more difficult. When the concentration of KI was increased to 0.75 mmol L^{-1} (0.50 mmol L^{-1} was sufficient, Figure S2), the capacitive arc in the low-frequency part disappeared. Especially, when it was applied together with GS, a stable protective layer was formed, which could even affect substances diffusion and cause a line representing the diffusion control process visible at the low-frequency region (because the shape of the curve in this part was random, it did not fit). Therefore, EIS data of the electrodes in the corrosive medium with 0.75 mmol L^{-1} KI were fitted utilizing the EEC in Figure 6 and the rests were fitted with that showed in Figure 3. The EEC parameters were presented in Table 5.

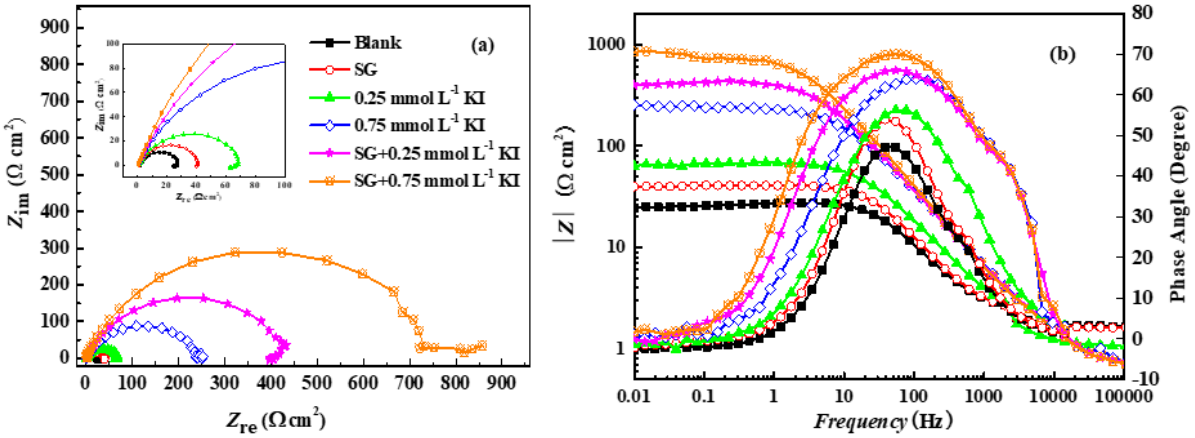

Figure 5. EIS of the electrodes in 0.5 mol L^{-1} H_2SO_4 solution without and with different corrosion inhibitor formulations: (**a**) Nyquist diagram; (**b**) Bode plots.

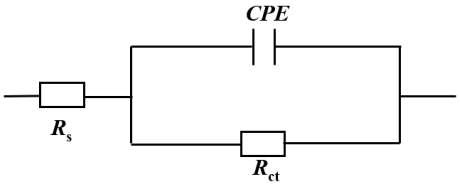

Figure 6. EEC to fit the EIS data for the electrodes in 0.5 mol L^{-1} H_2SO_4 solution with different corrosion inhibitor formulations.

Table 5. EIS fitting results for the electrodes in 0.5 mol L^{-1} H_2SO_4 solution with different corrosion inhibitor formulations.

Inhibitor Formulation	R_s (Ω cm^2)	$CPE-Y$ (μ Ω^{-1} cm^{-2} S^n)	$CPE-n$	R_{ct} (Ω cm^2)	R_L (Ω cm^2)	L (H cm^2)
Blank	1.67	643	0.76	30.5	121	7.68
GS	1.64	535	0.77	45.1	142	10.1
0.25 mmol L^{-1} KI	0.82	511	0.75	74.6	553	132
0.75 mmol L^{-1} KI	0.78	174	0.80	246	/	/
GS + 0.25 mmol L^{-1} KI	0.74	161	0.78	449	1.43×10^4	5.61×10^3
GS + 0.75 mmol L^{-1} KI	0.74	135	0.80	795	/	/

In Table 5, the most obvious point was that R_s was significantly reduced in the presence of KI, which should be ascribed to the addition of KI causing the ion's concentration in the solution to increase and the dielectric constant to decrease [25,26]. The value of $CPE-Y$ decreased, while R_{ct} increased when GS and/or KI was added in the system, implying that the adsorption of glucosamine molecules and/or iodide ions on the metallic surface changed the properties of the electric double layer. Thereby, the charge transfer became more difficult, and the carbon steel corrosion was suppressed [16,33]. Especially, the phenomenon was more significant in the case that KI and GS were applied together. It is clear that the value of R_{ct} increased by more than one order of magnitude compared with the blank; either GS was used with 0.25 mmol L^{-1} KI or 0.75 mmol L^{-1}, indicating that KI and GS had significant synergistic corrosion inhibitions.

3.3. Quantum Chemical Calculations

The adsorption performance of a corrosion inhibitor molecule strongly relies on its highest occupied molecular orbital (HOMO) and lowest unoccupied molecular orbital (LUMO), where HOMO is associated with its electron donation characteristics and LUMO is related to its electron acceptance behaviors [27,34–36]. Figure 7 presented the optimized structures of neutral and protonated glucosamine molecules, as well as their HOMO and LUMO distributions. For the neutral glucosamine molecule, HOMO was mainly distributed around the amino and carbonyl groups, indicating that these groups were easy to interact with the metals by providing negative charges from the heteroatoms of N and O. LUMO was mainly distributed in the carbonyl group, suggesting it was an active site for accepting electrons. When the glucosamine molecule was protonated, the LUMO distribution did not change much, but the location of HOMO was moved to the position almost complementary to LUMO, around the hydroxyl groups far away from the N atom. This was because that positive surplus charge existed around N as the amino group was protonated, which caused the active sites most likely to provide electrons alternating to the O atoms staying off N. The structural parameters of the related molecules were listed in Table 6. Global hardness (η), electronegativity (x), global softness (σ), nucleophilicity (ω), and the number of electrons transferred (ΔN) were calculated in line with the following relationships [5,35]:

$$\eta = (E_{LUMO} - E_{HOMO})/2 \quad (5)$$

$$x = -(E_{HOMO} + E_{LUMO})/2 \quad (6)$$

$$\sigma = 1/\eta \quad (7)$$

$$\omega = x^2/2\eta \quad (8)$$

$$\Delta N = (\phi_{Fe} - x)/2\eta \quad (9)$$

where E_{HOMO} was the energy of HOMO, and E_{LUMO} the energy of LUMO. ϕ_{Fe} was the work function and its value was 4.82 V, based on the experimental result [27,36,37].

E_{HOMO} represents the electron donation capability of an inhibitor molecule. A higher E_{HOMO} value suggests a stronger electron supply ability. It is notable that the electron donation capacity of the glucosamine molecule was weakened after protonation. E_{LUMO} reflects the electron acceptance capability of a molecule. A lower E_{LUMO} value indicates an easier electron acceptance process. After protonation, the E_{LUMO} of the glucosamine molecule was decreased, indicating that it got more prone to accept electrons from other substances for interaction. In addition, η measures the stability of itself. The lower its value is, the more unstable the inhibitor molecule is and the more easily it reacts with other substances. Thus, the higher η value of the pronated glucosamine molecule implied that it was more stable than the neutral one in the solution, which was consistent with the electrochemical experiment results. Furthermore, σ is the physical inverse of η. Generally, a neutral corrosion inhibitor is considered as Lewis's base and a higher value of σ indicates a better corrosion inhibition effect since it is easier to react with the soft acid (neutral metal). The protonated glucosamine molecule deserved the properties of hard Lewis's acid, and it

tended to interact with particles negatively charged. Ω can be used to evaluate the electrons attracting reactivity from a nucleophilic species. The higher ω value of the protonated glucosamine molecule demonstrated that it got more feasible to accept electrons in the solution [38,39]. The $\Delta N > 0$ suggests electron transfer from corrosion inhibitor molecules to metals, while the $\Delta N < 0$ indicates electron transfer from metals to organic compounds. Based on Table 6, the neutral glucosamine molecule interacted with the metal mainly by providing electrons to the metal and the protonated one via accepting negative charges.

Table 6. Quantum chemical parameters.

Compound	E_{HOMO} (eV)	E_{LUMO} (eV)	η (eV)	x (eV)	σ (eV^{-1})	ω (eV)	ΔN
Neutral Glucosamine	−6.91	−1.51	2.70	4.21	0.37	3.28	0.113
Protonated Glucosamine	−7.72	−1.94	2.89	4.83	0.35	4.04	−0.002

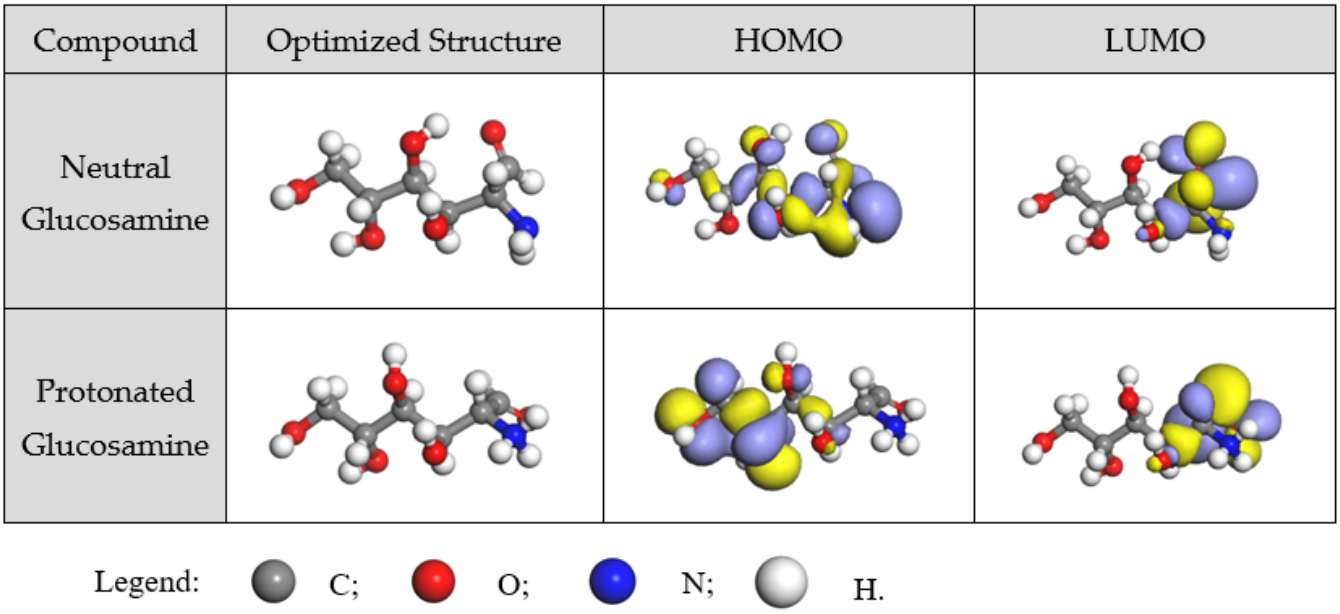

Figure 7. Optimized structures of neutral and protonated glucosamine molecules and their frontier molecular orbital density distributions.

3.4. Molecular Dynamics Simulations (MDS)

Compared with the experimental research, MDS can reveal the interaction mechanism of corrosion inhibitor molecules with the metal from the micro level, and is very helpful to elucidate the co-adsorption activities of different corrosion inhibitors [11–15]. Figure 8 provided the equilibrium adsorption configuration and adsorption energy of neutral and protonated glucosamine molecules on the Fe(110) surface, either with or without iodide ions. The adsorption energy E_{ads} of corrosion inhibitor on the solid surface was calculated according to the following formula [40,41]:

$$E_{ads} = E_{total} - (E_{surf + solu} + E_{inh}) \quad (10)$$

where E_{total} was the total energy of the adsorption system after adsorption, and $E_{surf + solu} + E_{inh}$ was the sum of the energy involved in the solid surface with the corrosive solution, as well as the corrosion inhibitor molecule before adsorption.

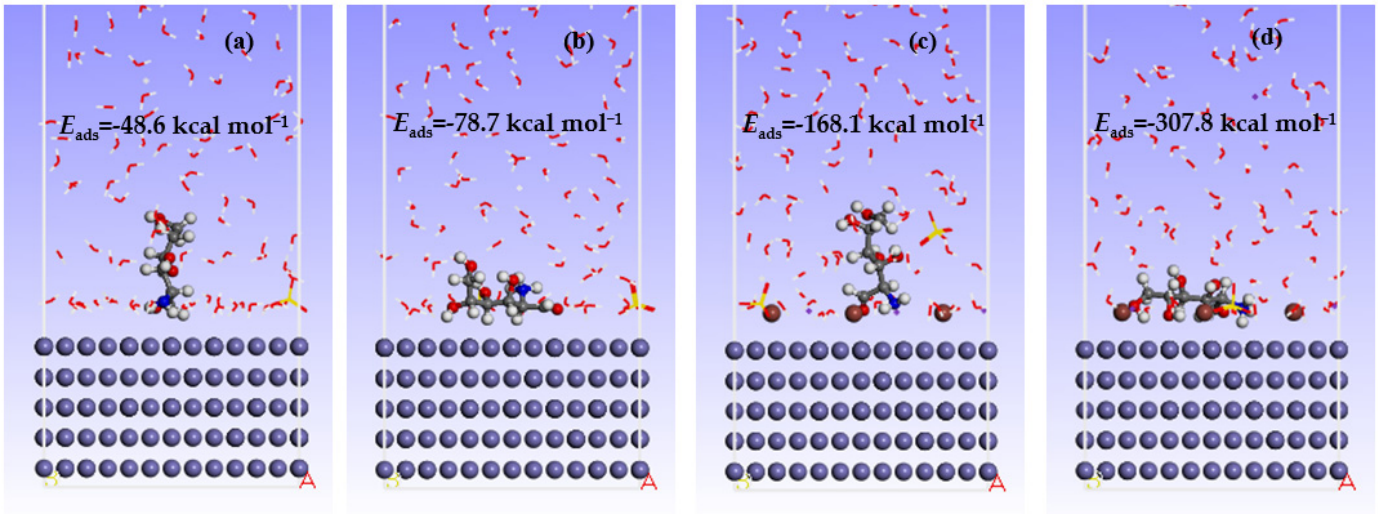

Figure 8. Equilibrium adsorption configurations of glucosamine molecules: (**a**) neutral glucosamine molecule on Fe(110) surface; (**b**) protonated glucosamine molecule on Fe(110) surface; (**c**) neutral glucosamine molecule on Fe(110) surface with idiom ions; (**d**) protonated glucosamine molecule on Fe(110) surface with idiom ions.

As can be inferred from Figure 8, the adsorption of the neutral glucosamine molecule on the solid surfaces was mainly through the amino and carbonyl groups. Based on Figure 7, it can be found that these sites were just consistent with the HOMO and LUMO distributions. The interaction at such a location meant that the glucosamine molecule adsorbed on the carbon steel surface not only by providing electrons to the d-empty orbital of iron, but also via accepting electrons. The protonated glucosamine molecule covered the solid surfaces parallelly. This type of configuration increased the interaction area of the corrosion inhibitor molecule with the solid surface; therefore, the adsorption of the protonated glucosamine molecule was much stronger than the neutral one. Yet, significant differences could be identified by comparing the adsorptions of protonated glucosamine molecules on the solid surface with and without iodide ions. At the Fe(110) surface free of iodide ions, the inhibitor molecule was adsorbed mainly by the action of the carbonyl group and hydroxyl group farthest from the amino group, whereas the protonated amino groups and other three hydroxyl groups were all upward and away from the metal surface. However, when iodide ions were presented, the protonated amino group became the most critical part for its interaction with the solid interface. Meanwhile, the glucosamine molecule also tried its best to adjust the conformation to enhance its adsorption on the solid surface, so that the carbonyl group and multiple hydroxyl groups all participated in the interaction. Furthermore, it is visible that E_{ads} of the protonated glucosamine molecule was far lower than that of the neutral one, either with iodide ions or not. This result indicated that the glucosamine molecule was prone to protonation in the acidic solution and interaction with the metal in such a style, which was totally in agreement with the research by other studies [16–18]. E_{ads} of the inhibitor molecule got much lower when iodide ions were presented, indicating a stronger interaction of the glucosamine molecule with the solid surface. Therefore, the synergistic inhibition effect of glucosamine molecules and iodide ions could be interpreted as follows: due to its oppositive charges with the metallic ions, iodide ions could first adsorb on the solid surface by forming a directional dipole, and then protonated inhibitor molecules were able to interact with the dipole by coulombic action; thus, glucosamine molecules could adsorb on the solid surface with halide ions as a bridge and inhibit the metal corrosion.

4. Conclusions

Corrosion inhibition characteristics of expired glucosamine drugs on carbon steel were examined by electrochemical tests. GH illustrated a good corrosion inhibition effect while GS exhibited low efficiency. However, the corrosion inhibition performance of GS could be greatly improved by iodide ions ascribed to their synergistic inhibition action. The corrosion inhibition efficiency reached above 90% when 2.5 mmol L^{-1} GS was applied together with 0.75 mmol L^{-1} KI. Glucosamine drugs were mixed-type corrosion inhibitors. Their inhibition properties were ascribed to the covering effect. Neutral glucosamine molecules could vertically adsorb on the metallic interface through the action of the amino and carbonyl groups, while interacting with the solid surface parallelly after protonation. Yet, the protonated glucosamine was difficult to adsorb on the metallic surface because it was positively charged in the acidic solution. By virtue of the opposite charges, halide ions favored galvanically coupled with the metallic cations and caused the solid surface to be negatively charged. Then, the protonated glucosamine molecules could absorb on the solid surface through the mediation of halide ions by electrostatic action, forming a tight anti-corrosion layer, and inhibiting the dissolution of carbon steel.

Supplementary Materials: The following supporting information can be downloaded at: https://www.mdpi.com/article/10.3390/cryst13020205/s1, Figure S1: EIS of carbon steel electrodes in 0.5 mol L^{-1} H_2SO_4 solution with 2.5 mmol L^{-1} GS in addition of various amounts of KI; Figure S2: EIS of carbon steel electrodes in 0.5 mol L^{-1} H_2SO_4 solution without and with various amounts of KI.

Author Contributions: Data curation, L.F., Y.Y. and Y.Z.; Investigation, L.F. and S.Z.; Visualization, R.P.; Writing—original draft, L.F. and S.Z.; Writing—review and editing, H.D. and Y.Y.; Supervision, F.L. All authors have read and agreed to the published version of the manuscript.

Funding: The APC was funded by Shandong Provincial Natural Science Foundation (No. ZR2019MEM046 and No.ZR2020QB084), the Science and Technology Development Plan Project of Weifang (No. 2020GX060), Doctoral Fund Project of Weifang University of Science and Technology (No. KJRC2022005 and No. KJRC2022006).

Data Availability Statement: The data presented in this study are available within the manuscript.

Acknowledgments: The authors gratefully acknowledge the financial support from Shandong Provincial Natural Science Foundation (No. ZR2019MEM046 and No.ZR2020QB084), the Science and Technology Development Plan Project of Weifang (No. 2020GX060), and the Doctoral Fund Project of Weifang University of Science and Technology (No. KJRC2022005 and No. KJRC2022006). The authors also specially thank the technical support in the chemical calculations and molecular simulations from National Supercomputer Center in Jinan and Institute of Metal Research, Chinese Academy of Sciences.

Conflicts of Interest: The authors declare no conflict of interest.

References

1. Eshwaran, R.; Kolibabka, M.; Poschet, G.; Jainta, G.; Zhao, D.; Teuma, L.; Murillo, K.; Hammes, H.P.; Schmidt, M.; Wieland, T.; et al. Glucosamine protects against neuronal but not vascular damage in experimental diabetic retinopathy. *Mol. Metab.* **2021**, *54*, 101333. [CrossRef] [PubMed]
2. Maruccia, E.; Lourenço, M.A.O.; Priamushko, T.; Bartoli, M.; Bocchini, S.; Pirri, F.C.; Saracco, G.; Kleitz, F.; Gerbaldi, C. Nanocast nitrogen-containing ordered mesoporous carbons from glucosamine for selective CO_2 capture. *Mater. Today Sustain.* **2022**, *17*, 100089. [CrossRef]
3. Mir, J.M.; Malik, B.A.; Khan, M.W. Glucosamine and maltol anchored Zinc(II) complex of COVID-19 health supplement relevance: DFT collaborated spectroscopic formulation with profound biological implications. *J. Indian Chem. Soc.* **2022**, *99*, 100743. [CrossRef]
4. Shintani, H.; Ashida, H.; Shintani, T. Shifting the focus of d-glucosamine from a dietary supplement for knee osteoarthritis to a potential anti-aging drug. *Hum. Nutr. Metab.* **2021**, *26*, 200134. [CrossRef]
5. Almashhadani, H.A.; Alshujery, M.K.; Khalil, M.; Kadhem, M.M.; Khadom, A.A. Corrosion inhibition behavior of expired diclofenac Sodium drug for Al 6061 alloy in aqueous media: Electrochemical, morphological, and theoretical investigations. *J. Mol. Liq.* **2021**, *343*, 117656. [CrossRef]

6. Tanwer, S.; Shukla, S.K. Recent advances in the applicability of drugs as corrosion inhibitor on metal surface: A review. *Curr. Res. Green Sustain. Chem.* **2022**, *5*, 100227. [CrossRef]
7. Wang, Y.; Qiang, Y.; Zhi, H.; Ran, B.; Zhang, D. Evaluating the synergistic effect of maple leaves extract and iodide ions on corrosion inhibition of Q235 steel in H_2SO_4 solution. *J. Ind. Eng. Chem.* **2023**, *117*, 422–433. [CrossRef]
8. Sherif, E.S.M.; Ahmed, A.H. Alleviation of Iron Corrosion in Chloride Solution by N,N′-bis[2-Methoxynaphthylidene] amino]oxamide as a Corrosion Inhibitor. *Crystals* **2021**, *11*, 1516. [CrossRef]
9. Zakaria, K.; Abbas, M.A.; Bedair, M.A. Herbal expired drug bearing glycosides and polysaccharides moieties as green and cost-effective oilfield corrosion inhibitor: Electrochemical and computational studies. *J. Mol. Liq.* **2022**, *352*, 118689. [CrossRef]
10. Feng, L.; Zhang, S.; Hao, L.; Du, H.; Pan, R.; Huang, G.; Liu, H. Cucumber (*Cucumis sativus* L.) Leaf Extract as a Green Corrosion Inhibitor for Carbon Steel in Acidic Solution: Electrochemical, Functional and Molecular Analysis. *Molecules* **2022**, *27*, 3826. [CrossRef]
11. Haruna, K.; Saleh, T.A.; Quraishi, M.A. Expired metformin drug as green corrosion inhibitor for simulated oil/gas well acidizing environment. *J. Mol. Liq.* **2020**, *315*, 113716. [CrossRef]
12. Sherif, E.S.M.; Ahmed, A.H.; Abdo, H.S.; DefAllah, M.N. Impediment of Iron Corrosion by N,N′-Bis[2-hydroxynaphthylidene] amino]oxamide in 3.5% NaCl Solution. *Crystals* **2021**, *11*, 1263. [CrossRef]
13. Chandrika, K.V.S.M.; Prathyusha, V. d-glucose and its analogue, d-glucosamine, as potential hydrogen storage materials: A quantum mechanical study. *Int. J. Hydrogen Energy* **2022**, *47*, 24014–24025. [CrossRef]
14. Tang, M.; Li, X.; Deng, S.; Lei, R. Synergistic inhibition effect of Mikania micrantha extract with KI on steel corrosion in H_2SO_4 solution. *J. Mol. Liq.* **2021**, *344*, 117926. [CrossRef]
15. Jeyaprabha, C.; Sathiyanarayanan, S.; Venkatachari, G. Influence of halide ions on the adsorption of diphenylamine on iron in 0.5M H_2SO_4 solutions. *Electrochim. Acta* **2006**, *51*, 4080–4088. [CrossRef]
16. Zhang, H.; Gao, K.; Yan, L.; Pang, X. Inhibition of the corrosion of X70 and Q235 steel in CO_2-saturated brine by imidazoline-based inhibitor. *Electroanal. Chem.* **2017**, *791*, 83–94. [CrossRef]
17. Ai, J.Z.; Guo, X.P.; Chen, Z.Y. The adsorption behavior and corrosion inhibition mechanism of anionic inhibitor on galvanic electrode in 1% NaCl solution. *Appl. Surf. Sci.* **2006**, *253*, 683–688. [CrossRef]
18. Wang, X.; Yang, H.; Wang, F. An investigation of benzimidazole derivative as corrosion inhibitor for mild steel in different concentration HCl solutions. *Corros. Sci.* **2011**, *53*, 113–121. [CrossRef]
19. Liu, S.; Xu, N.; Duan, J.; Zeng, Z.; Feng, Z.; Xiao, R. Corrosion inhibition of carbon steel in tetra-n-butylammonium bromide aqueous solution by benzotriazole and Na_3PO_4. *Corros. Sci.* **2009**, *51*, 1356–1363. [CrossRef]
20. Anaee, R.A.; Tomi, I.H.R.; Abdulmajeed, M.H.; Naser, S.A.; Kathem, M.M. Expired Etoricoxib as a corrosion inhibitor for steel in acidic solution. *J. Mol. Liq.* **2019**, *279*, 594–602. [CrossRef]
21. Rakhymbay, G.; Jumanova, R.; Avchukir, K.; Bakhytzhan, Y.; Argimbayeva, A.; Burkitbayeva, B.; Turmukhanova, M.; Vacandio, F.; Adeloye, A. Synthesis and evaluation of corrosion inhibitory and adsorptive properties of N-(beta-ethoxypropionitrile-N,N-bis(2-hydroxyethylethoxy) fatty amide. *R. Soc. Open Sci.* **2021**, *8*, 211066. [CrossRef] [PubMed]
22. Zhou, X.; Yang, H.; Wang, F. Investigation on the inhibition behavior of a pentaerythritol glycoside for carbon steel in 3.5% NaCl saturated $Ca(OH)_2$ solution. *Corros. Sci.* **2012**, *54*, 193–200. [CrossRef]
23. Qiu, Y.; Li, J.; Bi, Y.; Lu, X.; Tu, X.; Yang, J. Insight into synergistic corrosion inhibition of 3-amino-1,2,4-triazole-5-thiol (ATT) and NaF on magnesium alloy: Experimental and theoretical approaches. *Corros. Sci.* **2022**, *208*, 110618. [CrossRef]
24. Usman, B.J.; Umoren, S.A.; Gasem, Z.M. Inhibition of API 5L X60 steel corrosion in CO_2-saturated 3.5% NaCl solution by tannic acid and synergistic effect of KI additive. *J. Mol. Liq.* **2017**, *237*, 146–156. [CrossRef]
25. Sorkh Kaman Zadeh, A.; Shahidi Zandi, M.; Kazemipour, M. Corrosion protection of carbon steel in acidic media by expired bupropion drug; experimental and theoretical study. *J. Indian Chem. Soc.* **2022**, *99*, 100522. [CrossRef]
26. Tajabadipour, H.; Mohammadi-Manesh, H.; Shahidi-Zandi, M. Experimental and theoretical studies of carbon steel corrosion protection in phosphoric acid solution by expired lansoprazole and rabeprazole drugs. *J. Indian Chem. Soc.* **2022**, *99*, 100285. [CrossRef]
27. Dohare, P.; Chauhan, D.S.; Sorour, A.A.; Quraishi, M.A. DFT and experimental studies on the inhibition potentials of expired Tramadol drug on mild steel corrosion in hydrochloric acid. *Mater. Discov.* **2017**, *9*, 30–41. [CrossRef]
28. Zhu, H.; Chen, X.; Li, X.; Wang, J.; Hu, Z.; Ma, X. 2-aminobenzimidazole derivative with surface activity as corrosion inhibitor of carbon steel in HCl: Experimental and theoretical study. *J. Mol. Liq.* **2020**, *297*, 111720. [CrossRef]
29. Zheng, T.; Liu, J.; Wang, M.; Liu, Q.; Wang, J.; Chong, Y.; Jia, G. Synergistic corrosion inhibition effects of quaternary ammonium salt cationic surfactants and thiourea on Q235 steel in sulfuric acid: Experimental and theoretical research. *Corros. Sci.* **2022**, *199*, 110199. [CrossRef]
30. Ali, S.M.; Al Lehaibi, H.A. Control of zinc corrosion in acidic media: Green fenugreek inhibitor. *Trans. Nonferrous Met. Soc. China* **2016**, *26*, 3034–3045. [CrossRef]
31. Mohamed, K.E.M.; Ibrahim, O.H.; El-Bedawy, M.E.; Ali, A.H. Synergistic effect of different Zn salts with sodium octanoate on the corrosion inhibition of carbon steel in cooling water. *J. Radiat. Res. Appl. Sci.* **2020**, *13*, 276–287. [CrossRef]
32. Khadom, A.A.; Abd, A.N.; Ahmed, N.A. Synergistic effect of iodide ions on the corrosion inhibition of mild steel in 1 M HCl by Cardaria Draba leaf extract. *Results Chem.* **2022**, *4*, 100668. [CrossRef]

33. Liu, Y.; Wang, Z.; Chen, X.; Zhang, Z.; Wang, B.; Li, H.J.; Wu, Y.C. Synthesis and evaluation of omeprazole-based derivatives as eco-friendly corrosion inhibitors for Q235 steel in hydrochloric acid. *J. Environ. Chem. Eng.* **2022**, *10*, 108674. [CrossRef]
34. Feng, L.; Yang, H.; Wang, F. Experimental and theoretical studies for corrosion inhibition of carbon steel by imidazoline derivative in 5% NaCl saturated $Ca(OH)_2$ solution. *Electrochim. Acta* **2011**, *58*, 427–436. [CrossRef]
35. Obot, I.B.; Kaya, S.; Kaya, C.; Tüzün, B. Density Functional Theory (DFT) modeling and Monte Carlo simulation assessment of inhibition performance of some carbohydrazide Schiff bases for steel corrosion. *Phys. E Low Dimens. Syst. Nanostruct.* **2016**, *80*, 82–90. [CrossRef]
36. Xu, X.; Singh, A.; Sun, Z.; Ansari, K.R.; Lin, Y. Theoretical, thermodynamic and electrochemical analysis of biotin drug as an impending corrosion inhibitor for mild steel in 15% hydrochloric acid. *R. Soc. Open Sci.* **2017**, *4*, 170933. [CrossRef] [PubMed]
37. Olasunkanmi, L.O.; Obot, I.B.; Kabanda, M.M.; Ebenso, E.E. Some Quinoxalin-6-yl Derivatives as Corrosion Inhibitors for Mild Steel in Hydrochloric Acid: Experimental and Theoretical Studies. *J. Phys. Chem. C* **2015**, *119*, 16004–16019. [CrossRef]
38. Feng, L.; Yang, H.; Cui, X.; Chen, D.; Li, G. Experimental and theoretical investigation on corrosion inhibitive properties of steel rebar by a newly designed environmentally friendly inhibitor formula. *RSC Adv.* **2018**, *8*, 6507–6518. [CrossRef]
39. El-Hendawy, M.M.; Kamel, A.M.; Mohamed, M.M.A. The anti-corrosive behavior of benzo-fused N-heterocycles: An in silico study toward developing organic corrosion inhibitors. *Phys. Chem. Chem. Phys.* **2022**, *24*, 743–756. [CrossRef]
40. Song, Z.; Cai, H.; Liu, Q.; Liu, X.; Pu, Q.; Zang, Y.; Xu, N. Numerical Simulation of Adsorption of Organic Inhibitors on C-S-H Gel. *Crystals* **2020**, *10*, 742. [CrossRef]
41. Lgaz, H.; Chaouiki, A.; Chafiq, M.; Salghi, R.; Tachallait, H.; Bougrin, K.; Chi, H.Y.; Kwon, C.; Chung, I.M. Evaluating the corrosion inhibition properties of novel 1,2,3-triazolyl nucleosides and their synergistic effect with iodide ions against mild steel corrosion in HCl: A combined experimental and computational exploration. *J. Mol. Liq.* **2021**, *338*, 116522. [CrossRef]